Identification of Parameters in 2D-FEM of Valve Piping System within NPP Utilizing Seismic Response

Ruiyuan Xue[1], Shurong Yu[1, *] and Xiheng Zhang[1]

Abstract: Nuclear power plants (NPP) contain plenty of valve piping systems (VPS's) which are categorized into high anti-seismic grades. Tasks such as seismic qualification, health monitoring and damage diagnosis of VPS's in its design and operation processes all depend on finite element method. However, in engineering practice, there is always deviations between the theoretical and the measured responses due to the inaccurate value of the structural parameters in the model. The structure parameters identification of VPS within NPP is still an unexplored domain to a large extent. In this paper, the initial 2D-finite element model (FEM) for VPS with a DN80 gate valve was updated by utilizing seismic response. The objective function used in the model updating procedure is the vibration control equation error of the VPS. The experimental results show that the updated 2D-FEM can accurately predict the original dynamic characteristic of the VPS. It was also found the Rayleigh damping coefficients corresponding to the VPS vary slightly with the change in seismic excitation amplitude. The research displayed the complete procedure of updating the complex structured initial FEM by utilizing seismic response, and the results show that the parameters can be accurately identified even if the seismic response used for updating merely contained the fundamental frequency information of the structure.

Keywords: Seismic response, nuclear power plant, valve, FEM updating, parameter identification.

1 Introduction

With the deepening of people's awareness of seismic damage, new seismic requirements and regulations for systems and equipment in NPP have been proposed, for example, seismic margin analysis on in-service NPPs [Jha, Roshan, Pisharady et al. (2017); Oh, Kwag and Lee (2018)]. NPP contain plenty of VPS's which are categorized into high anti-seismic grades. In addition to economic factors, taking the following three reasons into consideration, seismic qualification on VPS's through shaking table could not always be carried out smoothly. First, experiments on in-service VPS's could not be carried out; second, layout design of VPS's and the determination of the seismic design value of substructures shall be accomplished in the design phase according to seismic qualification results; finally, limited by the size and performance of shaking table,

---

[1] College of Petrochemical Technology, Lanzhou University of Technology, Lanzhou, 730050, China.

* Corresponding Author: Shurong Yu. Email: yulut123@163.com; yusr@lut.edu.cn.

experiments could not be carried out on VPS's with larger size and quality, or the difficulty for boundary conditions to reflect in the test. In contrast, the FE method has the following advantages: on the one hand, seismic analysis based on the FE method could shorten seismic design period, save cost, and avoid damage of the experiment structure in extreme seismic capability test; on the other hand, a FEM which could accurately reflect the original dynamic characteristic of VPS is conductive to smooth implementation of health monitoring and damage diagnosis [Alkayem, Cao, Zhang et al. (2018); Eiras, Payan, Rakotonarivo et al. (2018)]. Thus, the FE method is the major approach to complete work related to VPS's seismic qualification in NPP.

Calculation of seismic response based on 3D-FEM requires a large amount of computational cost and storage space. The simplified FEM or 2D-FEM has less parameters and could extract structure response quickly, thus holds important position in the field of seismic analysis [Imai and Nakagawa (2012); Liu, Song and Wang (2020); Surh, Ryu, Park et al. (2015)]. In order to enhance the confidence in the seismic qualification on VPS's based on the analysis method, researchers have conducted many explorations on the calculation means of seismic responses [Liao, Ding and Li (2016); Surh, Ryu, Park et al. (2015)]. However, the above research did not pay attention to how to improve the relevance between 2D-FEM and actual structure. The seismic response of VPS's is quite sensitive towards its dynamic characteristic. There would always be parameters that are difficult to estimate accurately in the FEM of VPS, thereby leading to doubts in the matching between the dynamic characteristic of FEM and that of actual structure.

It is a common method in engineering practice to identify the material parameters [Qu, Xu and Jin (2010)], identify wireless multimedia device [Zhang, Li, Wang et al. (2018)] or infer goal and planning of agents [Wang, Wang, Zheng et al. (2018)] by using typical characteristics of research object. In the field of structural dynamics, the mode-based FEM updating method is generally used to identify the unknown parameters in the structure [Sabamehr, Lim and Bagchi (2018); Piao, Ouyang and Zhang (2020)]. Because it is difficult to accurately extract a sufficient number of modes of the systems and devices, the automatic FEM updating method has failed to be widely used in the seismic qualification field of NPP, but the ideology of FEM updating has been widely accepted [Cho, Kim and Chaudhary (2011); Park, Park, Lee et al. (2017)]. A simple and feasible automatic FEM updating method is urgently needed to identify structure parameters in FEMs of mechanical structures within NPP.

Compared with the modal data, acceleration responses are the VPS's-related dynamic test data more easily obtained in NPP, which are possibly derived from seismic responses that are monitored in the simulated operation test or in the service process. Wang et al. [Wang, Chi, Xie et al. (2020)] directly used the seismic response to identify the dynamic parameters of earth-rockfill dam, but the direct application of seismic response to identify the parameters in the mechanical structure has been rarely explored. Taking the vibration control equation error (VCEE) of the system as the objective function, a FEM updating method which can directly utilize the seismic response is proposed. The method is then used to update the 2D-FEMs of the VPS installed with DN80 gate valve in the horizontal and vertical directions. The existence of the valve presents a challenge for the establishment of the 2D-FEMs. This paper verifies the feasibility of using the VCEE-

based FEM updating method in the modeling process of complex mechanical structures, and verifies whether the 2D-FEM has the capability to accurately present the dynamic characteristic of the VPS.

2 Model updating theory derivation

When the VPS is subjected to seismic excitation, its VCEE in the frequency domain can be written as follows:

$$\boldsymbol{\varepsilon} = -\mathbf{M}\ddot{\mathbf{u}}_g - (\mathbf{M} + \mathrm{i}\omega^{-1}\mathbf{C} - \omega^{-2}\mathbf{K})\ddot{\mathbf{u}} \tag{1}$$

where $\mathbf{M}$, $\mathbf{C}$ and $\mathbf{K}$ respectively represent the mass matrix, damping matrix and stiffness matrix of VPS. $\ddot{\mathbf{u}}_g$ and $\ddot{\mathbf{u}}$ represent the vectors of seismic excitation and the seismic response in the frequency domain, $\ddot{\mathbf{u}}$ is the relative acceleration. Eq. (1) can be abbreviated as:

$$\boldsymbol{\varepsilon} = -\mathbf{M}\ddot{\mathbf{u}}_g - \mathbf{B}\ddot{\mathbf{u}} \tag{2}$$

$\mathbf{B}$ represents dynamic stiffness matrix. In essence, the FEM updating method proposed in this paper is a process of modifying a group of preselected parameters in the model to minimize $\boldsymbol{\varepsilon}$. Suppose $\boldsymbol{\theta}=\{\theta_1, \theta_2, \theta_3 \dots \theta_p\}^T$ is the updating parameters vector, p is the number of updating parameters. $\mathbf{M}$ and $\mathbf{B}$ are represented by the Taylor series expansion of updating parameters and all nonlinear terms are discarded. Then Eq. (2) translated into:

$$\boldsymbol{\varepsilon} = -\mathbf{M}_0\ddot{\mathbf{u}}_g - \mathbf{B}_0\ddot{\mathbf{u}} - \frac{\partial(\mathbf{M}\ddot{\mathbf{u}}_g + \mathbf{B}\ddot{\mathbf{u}})}{\partial\theta}\mathrm{d}\theta \tag{3}$$

Since the nonlinear terms are discarded, the $\boldsymbol{\theta}$ to minimize $\boldsymbol{\varepsilon}$ needs to be solved iteratively. Let $\mathrm{d}\boldsymbol{\theta}=\boldsymbol{\theta}_{i+1}-\boldsymbol{\theta}_i$, the subscript i indicates the current number of iteration. In this case, the iterative formula for $\boldsymbol{\theta}$ obtained by penalty function method can be found in Friswell et al. [Friswell and Mottershead (1995)]:

$$\boldsymbol{\theta}_{i+1} = \boldsymbol{\theta}_i + \left[\mathbf{A}^T\mathbf{A} + \mathbf{W}\right]^{-1}(\mathbf{A}^T\mathbf{b} - \mathbf{W}(\boldsymbol{\theta}_i - \boldsymbol{\theta}_0)) \tag{4}$$

where $\mathbf{W}$ is the inverse of the covariance matrix of the parameter estimates, which as a weighting matrix, provides less weight to parameters with a larger variation, $\boldsymbol{\theta}_0$ is the initial estimate vector of updating parameters. $\mathbf{b}$ and $\mathbf{A}$ are solved by the following equation:

$$\mathbf{b} = -\mathbf{M}_0\ddot{\mathbf{u}}_g - \mathbf{B}_0\ddot{\mathbf{u}} \tag{5}$$

$$\mathbf{A} = \frac{\partial\mathbf{B}}{\partial\boldsymbol{\theta}}\ddot{\mathbf{u}} + \frac{\partial\mathbf{M}}{\partial\boldsymbol{\theta}}\ddot{\mathbf{u}}_g \tag{6}$$

$\mathbf{A}$ is defined as the sensitivity matrix of updating parameters to VCEE. If $[\mathbf{A}^T\mathbf{A}]$ is singular or close to singular, Eq. (4) is often unable to solve or obtains solutions contrary to objective facts. Although Li et al. [Li, Cao, Chen et al. (2017)] proposed a more intelligent optimal value search algorithm. In order to simplify the calculation process, we still chose to add a positive definite matrix to $[\mathbf{A}^T\mathbf{A}]$ to improve the probability of

successful completion of the correction process, then Eq. (4) becomes:

$$\boldsymbol{\theta}_{i+1} = \boldsymbol{\theta}_i + \left[\mathbf{A}^T\mathbf{A} + \lambda\mathbf{e} + \mathbf{W} \right]^{-1} (\mathbf{A}^T\mathbf{b} - \mathbf{W}(\boldsymbol{\theta}_i - \boldsymbol{\theta}_0)) \qquad (7)$$

where λ is real constants and $\mathbf{e}$ is a p-order identity matrix. The value of λ needs to be adjusted according to the results of each iteration to make the updating process have the fastest convergence rate while ensuring that Eq. (7) can be solved smoothly. Eq. (7) is the final iterative mathematical model of the VCEE-based FEM updating method. From the above derivation, it can be seen that the method can identify parameters in FEM only by using the seismic response of VPS, and no modal information is involved in the updating process.

Through numerical simulation, we find that all the imaginary parts in the mathematical model must be discarded in order to obtain accurate updated results. Thus, the damping matrix of the VPS should be ignored during the update process. The frequency points used for updating should avoid the resonance frequency region to mitigate the effect of abandoning damping on the updated results, which is because the damping shows the highest sensitivity to the amplitude when the resonant frequency is reached. The damping matrix can be corrected separately after the mass and stiffness matrices have been accurately established, so as to match the measured and theoretical response peaks. This two-stage model updating strategy has been validated as feasible in many reports [Sipple and Sanayei (2014); Wang, Wang and Zhao (2017); Pradhan and Modak (2018)]. The flow chart of identifying the parameters in the FEM of mechanical structure by utilizing seismic response is shown in Fig. (1).
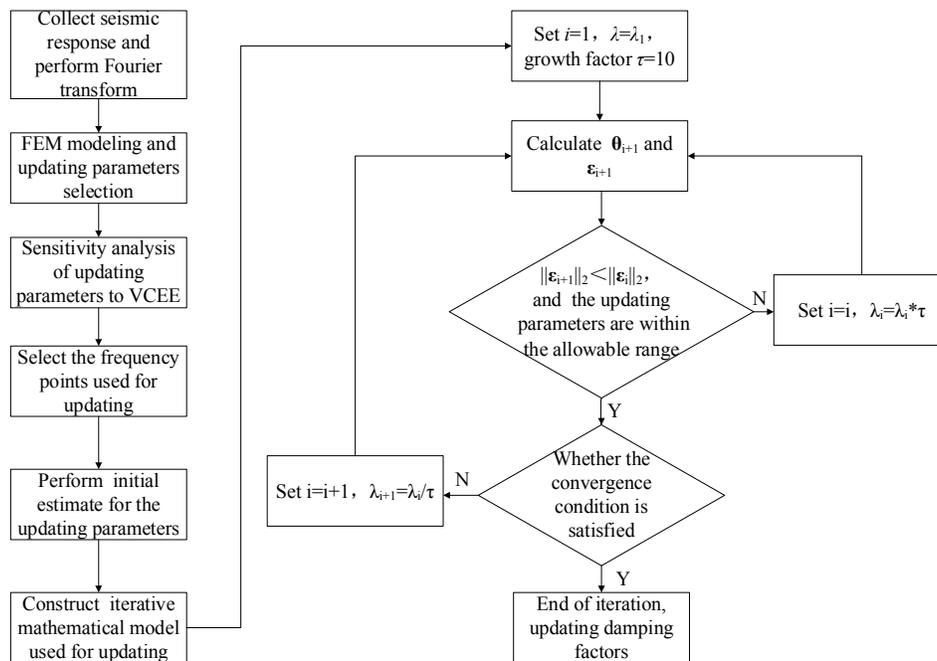
Figure 1: Flow chart of VCEE-based FEM updating method

3 Seismic simulation test of VPS and its establishment of 2D-FEM

3.1 Seismic response measurement

The main steam isolation valve piping system is a typical piping system installed with large quality valves in NPP. A VPS similar to the main steam isolation valve piping system is established, as shown in Fig. 2. The VPS consisting of a pipe of 2.326 m in length, a DN80 gate valve and a pipe of 0.815 m in length. The total length of the system is 3.445 m, and the mass of the valve takes up 80% of the overall system weight. The outer diameter and wall thickness of the pipe are 0.048 m×0.0035 m, the modulus of elasticity is $205×10^9$ Pa, and the weight is 3.78 kg/m. The two ends of the VPS are connected with the supports by nuts, and the supports are fixed on the shaking table by 8 M20 anchor bolts. The supports, welded by 0.003 m thick steel plates, have sufficient rigidity to transmit excitation of the shaking table to the VPS. The size of the shaking table with SDOF is 4 m×4 m and the maximum excitation frequency is 50 Hz. Different types of vibration tests are carried out by applying different forms of excitation to the VPS. During these tests, the responses of the system are measured by 16 accelerometers adsorbed on the system and the vibration time history of the shaking table is also monitored in real time.
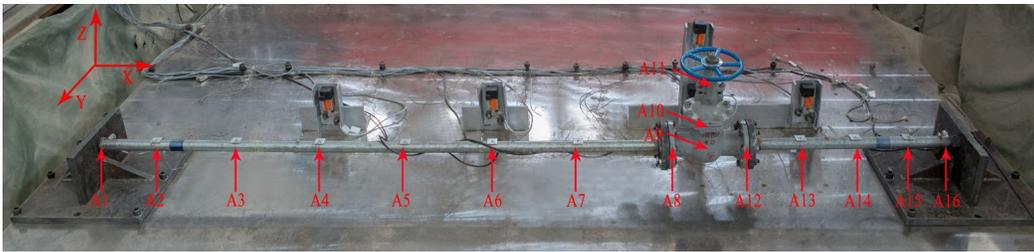
Figure 2: Details of the VPS and its acceleration measuring point arrangement

The test cases are shown in Tab. 1. Two types of tests were performed on the VPS. The acceleration response measured in Cases 2 and 5 were used to identify structure parameters in 2D-FEM corresponding to Y-direction and Z-direction VPS, respectively. The measurement data of Case 3 was used to verify the prediction ability of the updated model in the Y direction. Because the prediction ability of identification result has been verified in the Y direction, and in order to save the test cost, only one artificial seismic wave test was performed in the Z direction. The artificial seismic wave time history curves and its power spectral density (PSD) curves are shown in Fig. 3.

Fig. 4 draws the PSD curves of the responses measured during the white noise tests at the measuring points A_7, A_{11} and A_{14}. As shown in Fig. 4, in the Y direction, the VPS shows the three order natural frequencies within 50 Hz, which are 8.9 Hz, 30.5 Hz and 43.1 Hz respectively. Only two natural frequencies of 8.9 Hz and 39.7 Hz are displayed in the Z direction.

Table 1: Case details

Case No.	Excitation type	Motion duration	Direction	Excitation peak value
1	White noise	120 s	Y	1 m s^{-2}
2	Artificial seismic waves- I	60 s	Y	9 m s^{-2}
3	Artificial seismic waves- II	60 s	Y	12 m s^{-2}
4	White noise	120 s	Z	1 m s^{-2}
5	Artificial seismic waves- I	60 s	Z	9 m s^{-2}

(a) Time history curves   (b) PSD curves
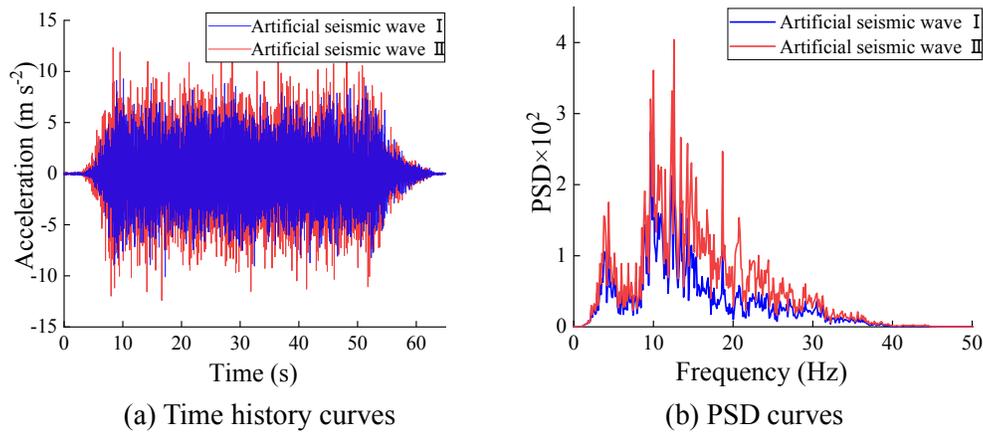
Figure 3: Time-frequency information of artificial seismic waves

3.2 2D-FEM establishment for the VPS

The beam elements and mass elements were used in the study to establish the 2D-FEM of the valve. The parameters with a clear physical significance, including length denoted as *L*, elastic modulus indicated as *E*, moment of inertia represented by *I* and cross-sectional area referred to as *A* of the beam element, equivalently replaced all uncertain factors associated with the valve. *L* could be set as the distance between the corresponding measurement points. The main task of modeling was to determine the value of *E*, *I* and *A*. The 2D-FEM established for the valve is shown in Fig. 5.

(a) Y direction   (b) Z direction
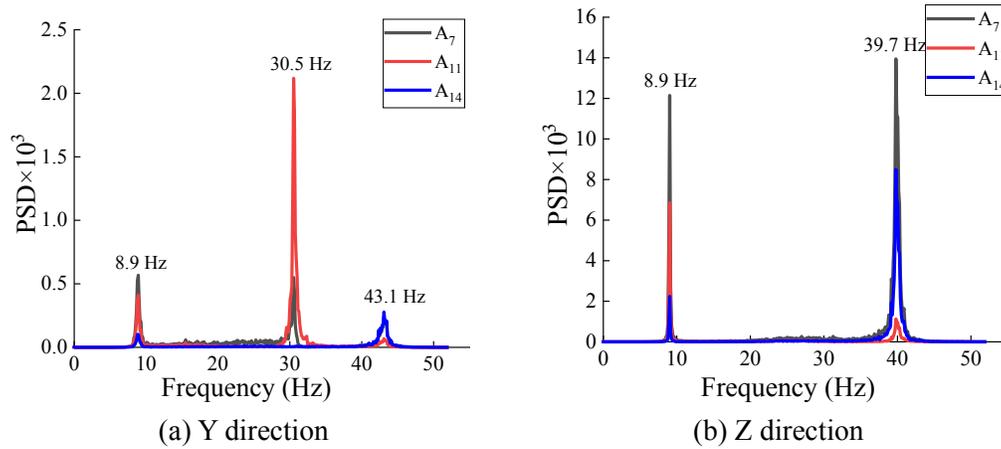
Figure 4: PSD curves measured by white noise test

The pipes were modeled using pipe elements, while the restraints of the supports on the system were modeled using linear springs. The lumped-mass FEM of the VPS as shown in Fig. 6, which is comprised of 11 pipe elements, 4 beam elements, 16 mass elements, and two linear springs. The position of each node corresponds to the position of the measuring points shown in Fig. 2.
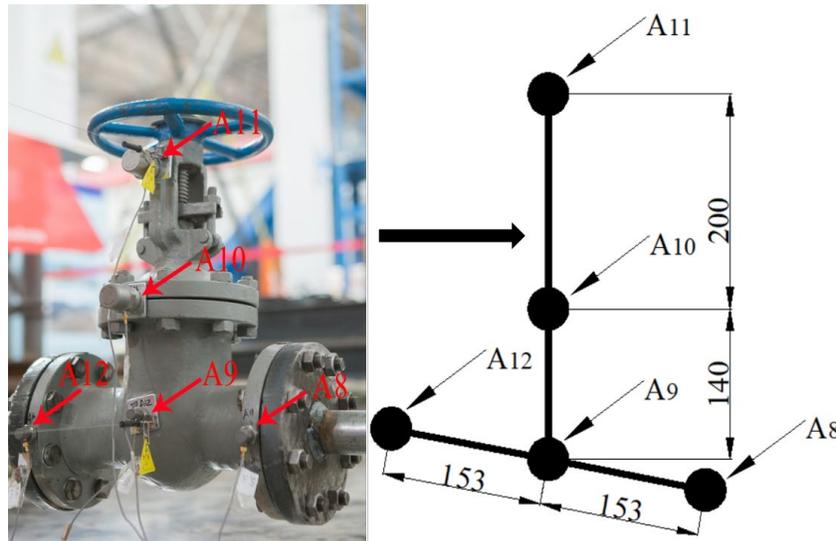
Figure 5: Lumped mass 2D-FEM corresponding to the valve (m)
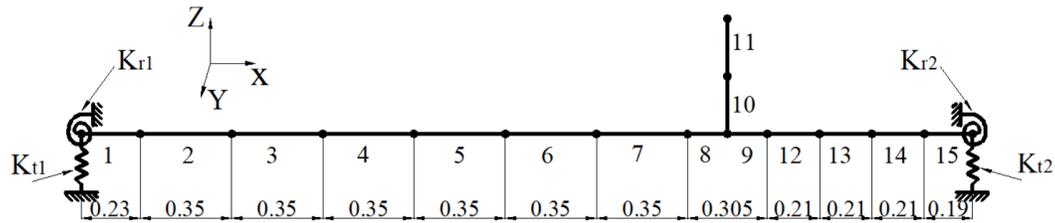
Figure 6: Lumped mass 2D-FEM corresponding to the VPS (m)

According to engineering experience, the translational stiffness K_t and rotational stiffness K_r of the linear spring, valve-related beam elements E, I and A and the mass assigned to each node are the main sources of the deviation between the FEM and the actual VPS. The above parameters can be regarded as updating parameters in the FEM updating process. The number of updating parameter is required to be further reduced to ensure the completion of correction. Firstly, based on past experience, the supports can provide sufficient constraints for the system in the horizontal direction, so that K_t could be considered as large enough. Secondly, the valve-related updating parameters were reduced by half through equivalent substitution, which means, placing the product of valve-related beam elements E and I with bending rigidity W_b, and replacing the product of E and A with compressive stiffness W_c. Finally, the mass of each node is required to be carefully allocated for the mass matrix of the system to be approximately determined.

The mass of the pipe elements was uniformly distributed to each node. The weight of each part of the valve is as follows. The valve body weighed 21.9 kg, the valve clack weighed 1.3 kg, the valve rod weighed 1 kg, the valve cover and stuffing box gland weighed 7.1 kg, the 8 bolts connecting the valve and cover weighed 1.3 kg, the hand wheel and fixed elements weighed 1.65 kg, the total weight of the valve weighed 34.25 kg, each bolt connecting the valve and the pipeline weighed 0.15 kg, and the flange welded to the pipeline weighed 5.1 kg. The mass of the valve body was evenly distributed across A_8, A_9, A_{10} and A_{12}, while the mass of the valve rod was evenly distributed across A_9, A_{10} and A_{11}. As the valve was closed, the mass of the valve clack was distributed at A_9. The mass of the bolt connecting the valve cover and valve body was distributed at A_{10}. The mass of the hand wheel and its fixed components was distributed at A_{11}. Due to the lower center of gravity, 1/3 mass of valve cover was distributed at A_{11}, with the rest at A_{10}. The mass of the eight bolts and flanges used at the end of the valve connected to the pipes were distributed in A_8 and A_{12}. In summary, the mass allocated to each node is shown in Tab. 2. The mass matrices in the Y and Z directions are identical.

Table 2: The mass assigned to each node

Measure point No.	1	2	3	4	5	6	7	8
Mass (kg)	0.29	1.24	1.34	1.34	1.34	1.34	1.34	12.46
Measure point No.	9	10	11	12	13	14	15	16
Mass (kg)	7.11	11.84	4.38	0.80	0.80	0.80	0.87	0.24

Elements 8 and 9 are symmetrical, so their parameter values can be considered equal. To sum up, in the 2D-FEMs corresponding to the VPS, the updating parameters in the Y-direction include: rotation stiffness of springs at the left and right end was K_{y1} and K_{y2}, bending rigidity of elements 8 and 9 in the Y direction was W_{by}, and the bending rigidity of elements 10 and 11 were W_{b10} and W_{b11}. The updating parameters in the Z-direction include: K_{z1} and K_{z2}, the rotation stiffness of springs at the left and right ends; W_{bz}, the bending rigidity of elements 8 and 9; as well as W_{c10} and W_{c11}, the compressive stiffness of elements 10 and 11.

4 Identification of uncertain parameters

4.1 Sensitivity analysis

The response of the VPS in the direction of rotational freedom was not measured during the test. Since the test structure was not subject to external excitation along the direction of rotation, static condensation could be performed on **K** in the initial FEM shown in Fig. 6 to obtain a condensed stiffness matrix **K'**, the rotational freedom of which was eliminated. **K'** was a 16-order matrix, and remained associated with the parameters in relation to the rotation freedom. The mass matrix used for updating was a 16-order diagonal matrix, and the diagonal elements are the mass assigned to each node shown in Tab. 2. The relative acceleration response of each measurement point can be obtained by subtracting the acceleration time history of the shaking table from the absolute acceleration response measured at each measurement point in Cases 2 and 5. Subsequently, the Fourier transform was performed on the relative acceleration responses and the acceleration time history of the shaking table to obtain **ü** and **ü$_g$**. By substituting the above mentioned results into Eqs. (1)-(7), an updating framework for the identification of structure parameters in the 2D-FEM could be established. The automatic updating process was achieved by means of programming in MATLAB.

Before executing the updating program, the sensitivity of the parameters to VCEE should be calculated to guide the selection of frequency points used for updating. The sensitivity of various parameters to VCEE along the Y and Z directions was calculated using Eq. (6), as shown in Fig. 7.

Fig. 7 indicates that the sensitivity of each parameter to the VCEE along the Y and Z directions has a similar trend, that is, the region with a lower sensitivity ranges from 5 Hz to 8.5 Hz and the maximum sensitivity was near the fundamental frequency. The sensitivity near the high-order natural frequency was close to zero, which is because the VPS only vibrates at the first-order natural frequency during the artificial seismic wave test. Due to the considerable effect of the measurement noise on low-frequency data, the sensitivity of each parameter shows a larger value below 5 Hz. In addition, below 5 Hz, the sensitivity of the Z-direction parameter to VCEE was significantly greater than the Y-direction one, which indicates that the measurement data along the Z-direction is affected more significantly by noise than along the Y-direction. It is worth noting that the sensitivity shown by the bending rigidity of elements 8 and 9 to VCEE exhibits a significant increase along the Z direction.
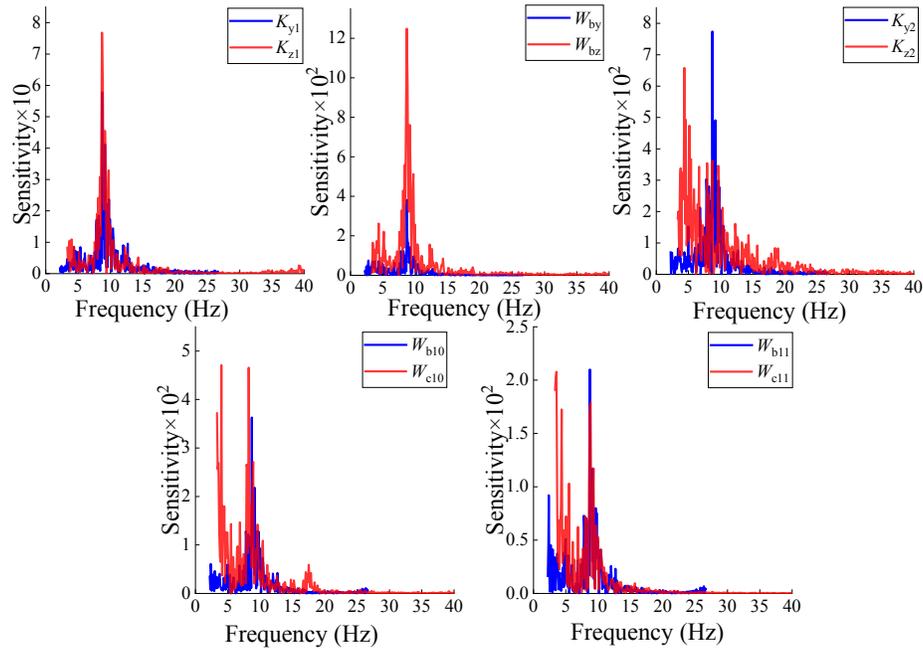
Figure 7: Sensitivity of each parameter to VCEE

4.2 Identification in Y direction

In this experiment, the impact of noise on the measured data showed a decreasing trend as the frequency is on the increase. The frequency points used for updating not only required avoiding the resonance frequency, but also the measurement data corresponding to these frequency points required enough accuracy. The frequency regions meeting this requirement are 5 Hz-8.5 Hz and more than 15 Hz. However, as the VPS vibrated at the first-order natural frequency, the frequencies above 15 Hz carry insufficient information about the dynamic characteristics, for which the frequency points were selected to be within 5 Hz-8.5 Hz. The principle applied to the further selection of frequency points in this region was that the initial VCEE calculated by Eq. (2) should be as small as possible.

In order to be consistent with the reality, it is assumed that only the measured fundamental frequency of the VPS is available before the updating. The initial estimates of the updating parameters were determined by the principle of theoretical and measured fundamental frequency coincidence. Each updating parameter has a specific physical meaning, but there is no engineering experience or criteria that can guide the order of magnitude for these parameters to be determined, for which each parameter should be changeable within a larger range. The allowable ranges of updating parameters are also determined according to the measured fundamental frequency. The theoretical fundamental frequency is significantly affected by all the updating parameters. In order to make the parameters have sufficient value space, it is required that the fundamental frequency calculated by the combination of parameters corresponding to the permissible lower and upper limits is either slightly less and greater than the testing results. The initial estimate information and updated results of the updating parameters in the Y-

direction FEM of the VPS are shown in Tab. 3.

Table 3: Identification results of uncertain parameters in Y-direction

Updating parameters	Frequency points participate in identification	Initial estimation	Variation range	Identification results
K_{y1} (N mrad^{-1})		1.50e5	9.00e4-3.00e5	1.53e5
K_{y2} (N mrad^{-1})	5.71 Hz, 5.88 Hz,	1.50e5	9.00e4-3.00e5	1.46e5
W_{by} (N m^6)	5.96 Hz,	9.00e4	1.00e4-1.00e5	1.89e4
W_{b10} (N m^6)	6.21 Hz, 6.22 Hz	9.00e4	2.00e3-1.00e5	4.17e3
W_{b11} (N m^6)		9.00e4	2.00e3-1.00e5	2.53e3

As shown in Tab. 3, the identification results of K_{y1} and K_{y2} are slightly different. It was because the nuts connecting the pipes and the supports were processed and tightened manually. In addition, the bending rigidity of each beam element used to simulate the valve is not equal and significantly smaller than initially estimated. For engineering applications, if the valve is set as a mass point and rigidly connected to the pipeline, the analytical result will show a considerable deviation from the actual situation.

The natural frequencies of the first three orders corresponding to the updated 2D-FEM are 8.96 Hz, 29.7 Hz and 43.6 Hz, the deviation of which from the test results were 0.67%, 2.29%, and 1.16%, respectively. The high-frequency information was excluded from the response used for updating, but the updated 2D-FEM remained capable to accurately predict the high-order natural frequencies of the VPS, which is a significant advantage of the VCEE-based FEM updating method. That is to say, the required response data removes the need to include the higher-order mode, which could ensure that the test data for updating is easily obtainable.

Certainly, the reliability of the identification results also requires to be validated by the degree of matching between the theoretical and experimental seismic responses. It is essential to set accurate damping for the system prior to calculating the seismic response. Rayleigh damping is widely used to simulate the energy dissipation mechanism of the systems and equipment in NPPs. In terms of the VPS, there is invariably a deviation between the peak of the seismic response corresponding to the theoretical damping coefficient and the actual result and the presence of the valve makes the damping distribution of the system show the clearly non-proportional. If the deviation is within the acceptable range, it can be reduced by updating the damping coefficients, otherwise it is necessary to re-identify the updating parameters.

The impact of damping is limited to the amplitude of the response. Many scholars achieved a success in matching the measured and theoretical FRF curve peaks quickly by updating the damping ratio manually [Sipple and Sanayei (2014); Wang, Wang and Zhao (2017)]. The damping coefficients of different parts of the VPS are also mutually independent, for which a manual updating method was applied to update the damping coefficients of the system. As the measured responses of A_1 and A_{16} was greatly affected by noise, the measured maximum response of A_2-A_{15} was taken as the objective to manually update the damping coefficients set for different parts of the VPS. The results

are presented in Tab. 4, where α and β represent the mass damping coefficient and the stiffness damping coefficient respectively.

Table 4: Damping updated result by using test data of case 1 in Y-direction

Element No.	1, 2, 3, 4, 5, 6, 7		8, 9, 10, 11		12, 13, 14, 15	
Damped coefficient	α	β	α	β	α	β
Correction results	0.8	2e-5	3.5	4e-4	0.8	1e-4

In order to verify the capability of the updated FEM to reproduce the seismic response used for parameter identification, the A_5 and A_7 at the longer pipe, the valve related measurement points A_8-A_{12} and the A_{14} at the shorter pipe were selected to compare the measured and theoretical responses. Fig. 8 shows the overlap of the measured and theoretical PSD curves.

As shown in Fig. 8, the resonance frequency exhibited by the PSD curve as calculated using the updated model is excellently consistent with the experimental result. In addition, as the damping coefficients had been manually updated meticulously, the resonance peaks of the two PSD curves were shown to be basically identical.
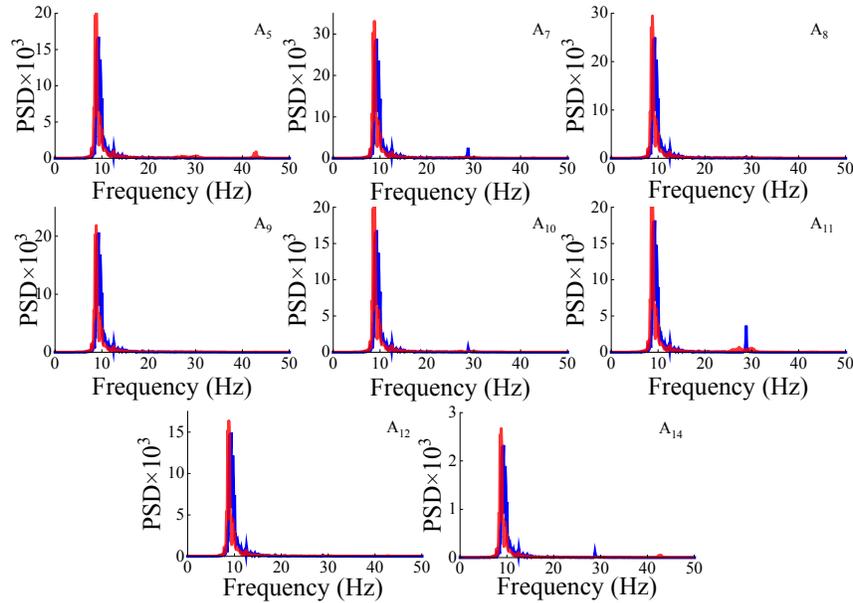
Figure 8: Comparison of PSD curves between theoretical (represented by a blue line) and measured (represented by a red line) of the VPS under the artificial seismic wave-I in Y-direction

The updated model reproduces the seismic response. The theoretical and measured responses of the VPS under the effect of artificial seismic wave II were compared to demonstrate that the updated 2D-FEM is capable to predict the seismic response of the VPS under different conditions of excitation. Nevertheless, it was found out that the

amplitude of the theoretical response was greater when compared to the measured result. Therefore, with the maximum response of A_2-A_{15} measured in case 3 as the target, the damping coefficients of each part of the VPS were manually updated again. The updated results are shown in Tab. 5.

Table 5: Damping updated result by using test data of case 3 in Y-direction

Element No.	1, 2, 3, 4, 5, 6, 7		8, 9, 10, 11		12, 13, 14, 15	
Damped coefficient	α	β	α	β	α	β
Correction results	1.2	6e-5	3.5	5.5e-4	1.2	3e-4

As revealed by the comparison drawn between Tabs. 4 and 5, the Rayleigh damping coefficients corresponding to the VPS show an insignificant increase as the excitation amplitude is on the rise. The re-updated damping coefficients were assigned to the updated model for the seismic response under the Case 3 to be re-predicted. Fig. 9 presents the comparison of PSD curves between the measured and theoretical response of the VPS under the excitation of artificial earthquake wave II.
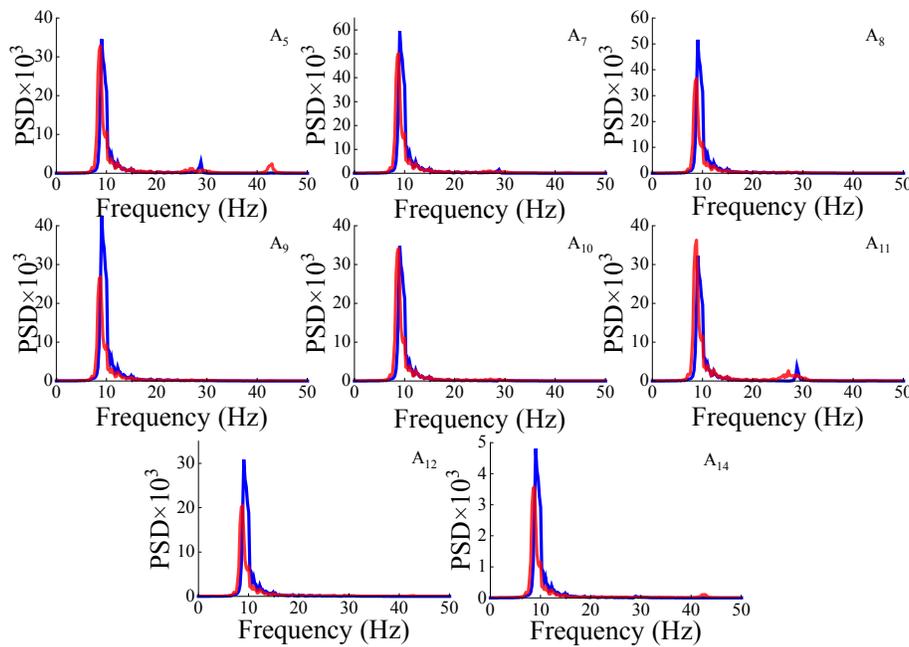
Figure 9: Comparison of PSD curves between theoretical (represented by a blue line) and measured (represented by a red line) of the VPS under the artificial seismic wave- II in Y-direction

As shown in Fig. 9, after the damping coefficients are updated again, under the excitation of artificial seismic wave II, the PSD curve for each measurement point as obtained by theoretical analysis is broadly consistent with the measurement result in respect of waveform. However, the relatively conservative theoretical resaults were obtained for A_8,

A_9 and A_{12} located at the horizontal part of the valve body, which is attributed to the differences between Rayleigh damping and the actual energy consumption mechanism of the system, rather than the inaccurate identification results

4.3 Identification in Z direction

Due to the noticeable increase of W_{bz} sensitivity to VCEE, when the frequency combination shown in Tab. 3 were applied to identify the parameters along the Z-direction, λ was assigned a larger value for the purpose of ensuring that W_{bz} would change within a reasonable range. Consequently, only W_{bz} changed at each time of iteration. Therefore, it is essential to increase the value of the frequencies used for updating to enhance the sensitivity of other parameters to VCEE. In addition, the measured data in Z direction are greatly affected by noise, and the accuracy of the measured data can be ensured by choosing higher frequency points. Meanwhile, the initial estimation of updating parameters should be as accurate as possible to ensure the smooth completion of the correction process. Taking the theoretical and measured fundamental frequencies as the goal and referring to the updated results in the Y direction, the initial estimation of the parameters in the Z direction is made. The initial estimate information and final updated results of the updating parameters in the Z-direction FEM of the VPS are shown in Tab. 6.

Table 6: Identification results of uncertain parameters in Z-direction

Updating parameters	Frequency points participate in identification	Initial estimation	Variation range	Identification results
K_{z1} (N mrad^{-1})		1.50e5	9.00e4-3.00e5	1.52e5
K_{z2} (N mrad^{-1})	7.84 Hz, 8.00 Hz,	1.50e5	9.00e4-3.00e5	1.48e5
W_{bz} (N m^6)	8.22 Hz,	5.00e4	4.00e4-1.00e5	4.03e4
W_{c10} (N m^4)	8.38 Hz, 8.53 Hz	2.00e6	1.00e6-3.00e6	1.75e6
W_{c11} (N m^4)		2.00e5	1.00e5-3.00e5	1.77e5

As indicated by Tab. 6, K_{y1}, K_{y2} and K_{z1}, K_{z2} are basically the same, which indicates that the supports provide the identical constraint for the VPS in the Y and Z directions. Besides, the bending rigidity of elements 8 and 9 in the Z direction is greater than in the Y direction. Elements 10 and 11 exhibited compressive stiffness in the Z direction, as a result of which W_{c10} and W_{c11} showed a larger value. The natural frequencies of the first two orders corresponding to the updated 2D-FEM in the Z-direction were 8.94 Hz and 38.5 Hz, the deviation of which from the experimental results is 0.45% and 3.02%, respectively. The damping coefficients in the Z direction were manually updated in the same way, the results are shown in Tab. 7.

So far, the construction of the 2D-FEM of the VPS in the Z direction has been complete. The comparison performed between the measured and theoretical response results of the Z-direction VPS under the effect of artificial seismic wave I is illustrated in Fig. 12.

Table 7: Damping updated result by using test data of case 6 in Z-direction

Element No.	1, 2, 3, 4, 5, 6, 7		8, 9, 10, 11		12, 13, 14, 15	
Damped coefficient	α	β	α	β	α	β
Correction results	1	8e-5	3.5	2.5e-4	1	8e-5

As shown in Fig. 12, the measured PSD curve corresponding to A_{11} has relatively larger amplitude within 4 Hz due to the effect of noise. Despite this, the resonance frequency and the amplitude at the resonant frequency shown by the PSD curves of the theoretical and experimental measurement points exhibited a remarkable consistence, which suggests that the updating parameters in the 2D-FEM along the Z direction were precisely identified using the seismic response.
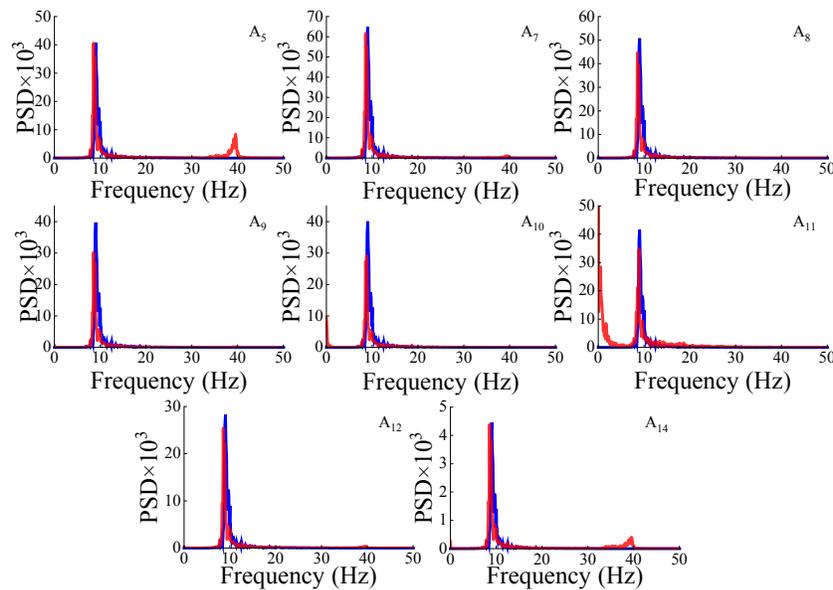
Figure 12: Comparison of PSD curves between theoretical (represented by a blue line) and measured (represented by a red line) of the VPS under the artificial seismic wave-I in Z-direction

5 Conclusion

Based on the VCEE as the objective function, a FEM updating method which can identify the structural parameters in the VPS directly by seismic response is proposed. Subsequently, the initial FEM of the VPS whose 80% of its total mass is comprised of valve was updated with the method, and the prediction ability of the updated model was verified. The following conclusions were drawn:

1, The VCEE-based FEM updating method avoids the use of modes and provides a simple way for the identification of unknown structural parameters of VPS's within NPP. A major advantage of the method is that the structure parameters of VPS can be

accurately identified even if the seismic response for the updating contains only the fundamental frequency information, hence greatly lowering the difficulty in which the test data needed for updating can be obtained.

2, 2D-FEMs have the ability to accurately predict the dynamic characteristics of VPS's. It is important that the valve and pipe are not rigidly connected in the 2D-FEM. The physical parameters of the beam elements used to simulate the valve must be identified by the FEM updating method.

3, The computation simplicity of Rayleigh damping have given it an edge in its anti-seismic applications for NPP, but this experiment has shown that it is possible for the Rayleigh damping coefficients corresponding to a VPS to increase slightly with the increase of excitation amplitude. NPPs tend to adopt conservative measures due to safety reasons, a theoretical result that is greater than the measured value is acceptable. The updated damping coefficients should be appropriately reduced when using the updated model to predict the responses under a seismic excitation that is smaller than that used in the identification process.

Conflicts of Interest: The authors declare that they have no conflicts of interest to report regarding the present study.

References

Alkayem, N. F.; Cao, M.; Zhang, Y. F.; Bayat, M.; Su, Z. Q. (2018): Structural damage detection using finite element model updating with evolutionary algorithms: a survey. *Neural Computing and Applications*, vol. 30, pp. 389-411.

Cho, S. G.; Kim, D.; Chaudhary, S. (2011): A simplified model for nonlinear seismic response analysis of equipment cabinets in nuclear power plants. *Nuclear Engineering and Design*, vol. 241, pp. 2750-2757.

Eiras, J. N.; Payan, C.; Rakotonarivo, S.; Garnier, V. (2018): Experimental modal analysis and finite element model updating for structural health monitoring of reinforced concrete radioactive waste packages. *Construction and Building Materials*, vol. 180, pp. 531-543.

Friswell, M. I.; Mottershead, J. E. (1995): Finite element model updating in structural dynamics. Springer, Dordrecht. https://doi.org/10.1155/2018/5264526.

Imai, R.; Nakagawa, M. (2012): A reduction algorithm of contact problems for core seismic analysis of fast breeder reactors. *Computer Modeling in Engineering & Sciences*, vol. 84, no. 3, pp. 253-282.

Jha, S.; Roshan, A. S.; Pisharady, A. S.; Bishnoi, L. B. (2017): Seismic margin assessment for earthquake beyond design basis-simplified practical approach. *Nuclear Engineering and Design*, vol. 323, pp. 329-337.

Li, W. J.; Cao, Y. X.; Chen, J.; Wang, J. X. (2017): Deeper local search for parameterized and approximation algorithms for maximum internal spanning tree. *Information and Computation*, vol. 252, pp. 187-200.

Liao, C. W.; Ding, W.; Li, F. (2016): An improved algorithm for numerical calculation of seismic response spectra. *Geodesy and Geodynamics*, vol. 7, no. 2, pp. 148-155.

Liu, W.; Song, Z.; Wang, Y. (2020): Seismic analysis of the connections of buried segmented pipes. *Computer Modeling in Engineering & Sciences*, vol. 123, no. 1, pp. 257-282.

Oh, J.; Kwag, S.; Lee, J. (2018): A new design concept and seismic margin assessment for a spent fuel storage system. *Nuclear Engineering and Design*, vol. 326, pp. 150-161.

Park, J. B.; Park, N. C.; Lee, S. J.; Park, Y. P.; Choi, Y. (2017): Seismic analysis of the APR1400 nuclear reactor system using a verified beam element model. *Nuclear Engineering and Design*, vol. 313, pp. 108-117.

Piao, S.; Ouyang, H.; Zhang, Y. (2020): Beam approximation for dynamic analysis of launch vehicles modelled as stiffened cylindrical shells. *Computer Modeling in Engineering & Sciences*, vol. 122, no. 2, pp. 571-591.

Pradhan, S.; Modak, S. V. (2018): A two-stage approach to updating of mass, stiffness and damping matrices. *International Journal of Mechanical Sciences*, vol. 140, pp. 133-150.

Qu, J.; Xu, B.; Jin, Q. (2010): Parameter identification method of large macro-micro coupled constitutive models based on identifiability analysis. *Computers, Materials & Continua*, vol. 20, no. 2, pp. 119-158.

Sabamehr, A.; Lim, C.; Bagchi, A. (2018): System identification and model updating of highway bridges using ambient vibration tests. *Journal of Civil Structural Health Monitoring*, vol. 8, pp. 755-771.

Sipple, J. D.; Sanayei, M. (2014): Finite element model updating of the UCF grid benchmark using measured frequency response functions. *Mechanical Systems and Signal Processing*, vol. 246, no. 1, pp. 179-190.

Surh, H. B.; Ryu, T. Y.; Park J. S.; Ahn, E. W.; Choi, C. S. et al. (2015): Seismic response analysis of a piping system subjected to multiple support excitations in a base isolated NPP building. *Nuclear Engineering and Design*, vol. 292, pp. 283-295.

Wang, J. T.; Wang, C. J.; Zhao, J. P. (2017): Frequency response function-based model updating using kriging model. *Mechanical Systems and Signal Processing*, vol. 87, pp. 218-228.

Wang, M. H.; Chi, S. C.; Xie, Y. F.; Zhou, X. X. (2020): Dynamic parameters inversion analysis of rockfill materials considering interaction effects based on weak earthquakes. *Soil Dynamics and Earthquake Engineering*, vol. 130, pp. 1-14.

Wang, X. F.; Wang, L.; Zheng, Y. H.; Wang, J. (2018): An event-driven plan recognition algorithm based on intuitionistic fuzzy theory. *Journal of Supercomputing*, vol. 74, no. 12, pp. 6923-6938.

Zhang, Z.; Li, Y. B.; Wang, C.; Wang, M. Y.; Tu, Y. et al. (2018): An ensemble learning method for wireless multimedia device identification. *Security and Communication Networks*. https://doi.org/10.1155/2018/5264526.